

University of Groningen

Adaptation after mild traumatic brain injury

van der Horn, Harm

IMPORTANT NOTE: You are advised to consult the publisher's version (publisher's PDF) if you wish to cite from it. Please check the document version below.

Document Version

Publisher's PDF, also known as Version of record

Publication date:

2017

[Link to publication in University of Groningen/UMCG research database](#)

Citation for published version (APA):

van der Horn, H. (2017). *Adaptation after mild traumatic brain injury: The role of structural and functional brain networks*. [Thesis fully internal (DIV), University of Groningen]. Rijksuniversiteit Groningen.

Copyright

Other than for strictly personal use, it is not permitted to download or to forward/distribute the text or part of it without the consent of the author(s) and/or copyright holder(s), unless the work is under an open content license (like Creative Commons).

The publication may also be distributed here under the terms of Article 25fa of the Dutch Copyright Act, indicated by the "Taverne" license. More information can be found on the University of Groningen website: <https://www.rug.nl/library/open-access/self-archiving-pure/taverne-amendment>.

Take-down policy

If you believe that this document breaches copyright please contact us providing details, and we will remove access to the work immediately and investigate your claim.

Downloaded from the University of Groningen/UMCG research database (Pure): <http://www.rug.nl/research/portal>. For technical reasons the number of authors shown on this cover page is limited to 10 maximum.

4.

Altered Wiring of The Human Structural Connectome in Adults with Mild Traumatic Brain Injury

Harm J. van der Horn, MD¹; Jelmer G. Kok, MD¹; Myrthe E. de Koning, BSc¹; Myrthe E. Scheenen, MSc²; Alexander Leemans, PhD³; Jacoba M. Spikman, PhD²; Joukje van der Naalt, MD, PhD¹

¹Department of Neurology, University of Groningen, University Medical Center Groningen, The Netherlands

²Department of Neuropsychology, University of Groningen, University Medical Center Groningen, The Netherlands

³Image Sciences Institute, University Medical Center Utrecht, The Netherlands

J Neurotrauma 2017 Mar 1; 34(5): 1035-1044

Abstract

In this study, structural connectivity after mild traumatic brain injury (mTBI) was examined from a network perspective, with a particular focus on post-traumatic complaints. Fifty-three patients with and without self-reported complaints at two weeks after uncomplicated mTBI were included in addition to 20 matched healthy controls. Diffusion weighted imaging was performed at four weeks post-injury, and neuropsychological tests measuring processing speed and verbal memory were administered at three months post-injury to determine cognitive outcome. Structural connectivity was investigated using whole brain tractography and subsequent graph theory analysis. In patients with mTBI, eigenvector centrality within the left temporal pole was lower compared to healthy controls. In patients without complaints, global and mean local efficiency were lower compared to patients with complaints, although no differences were found between either subgroup and the group of healthy controls. Neuropsychological test scores were similar for patients with mTBI and healthy controls. However, patients with complaints showed higher processing speed compared to patients without complaints. Within the total mTBI group, a trend was found toward a correlation between lower network clustering and higher processing speed. Additionally, significant correlations were found between higher betweenness centrality values of language areas and lower verbal memory scores in patients with mTBI. In conclusion, our findings may indicate that global graph measures of the structural connectome are associated with pre- and/or non-injury related factors that determine the susceptibility to develop (persistent) complaints after mTBI.

Furthermore, correlations between graph measures and neuropsychological test scores could suggest early compensatory mechanisms to maintain adequate cognitive performance.

Introduction

Mild traumatic brain injury (mTBI) occurs frequently worldwide, and may result in post-traumatic cognitive and affective complaints that persist long beyond the accident in a quarter of patients (Dischinger et al. 2009; Ettenhofer & Barry 2012; Ponsford et al. 2011; de Koning et al. 2016; Cassidy et al. 2014). However, in most cases cognitive impairments cannot be objectified by neuropsychological testing (Carroll et al. 2004). Moreover, there is an ongoing debate as to whether these complaints are related to structural injury since in general no correlations have been found with findings from clinical neuroimaging modalities, such as computed tomography (CT) and conventional magnetic resonance imaging (MRI) (Bazarian et al. 2006; Iverson et al. 2000; Yuh et al. 2013).

Diffusion tensor imaging (DTI) has been used in multiple studies of mTBI to study white matter (Dodd et al. 2014). However, findings so far vary significantly, especially regarding the anatomical location and direction of changes in diffusion parameters (e.g. fractional anisotropy (FA) and mean diffusivity (MD)) (Dodd et al. 2014). A recent DTI study has shown that diffusion parameters were similar for acute mTBI and healthy control subjects (Ilvesmaki et al. 2014). Furthermore, in instances of diffusion changes after mTBI, the relationship with post-traumatic complaints is unclear. In fact, recent DTI studies have not shown differences in diffusion parameters between patients with and without complaints (Ilvesmaki et al. 2014; Lange et al. 2015; Wäljas et al. 2014), which casts doubts on the influence of structural injury on the development of complaints after mTBI.

Most of the conducted DTI studies on mTBI have used methods that detect changes in diffusion parameters, either in regions of interest or in white-matter skeletons (Dodd et al. 2014; Jones & Cercignani 2010). It could be argued that modeling white matter tracts as a network (i.e. connectome) results in a better approximation of the brain's complex topological features and of interactions between regions (Filippi et al. 2013; Sharp et al. 2014; Sporns 2013). Especially in a heterogeneous condition such as mTBI, studying connectivity of structural networks may be valuable for exposing patterns of white matter alterations that remain latent with traditional methods that have been used so far. In this context, networks (or graphs) are defined by their anatomical regions (nodes) and connections between regions (edges), which may be weighted, for example, by the number of reconstructed streamlines. Subsequently, graph theory can be applied (Rubinov & Sporns 2010). With this method various graph measures can be calculated to study characteristics of the whole network or its individual nodes. Graph theory measures are subdivided into three main domains: Integration, Segregation and Influence (Sporns 2013). Integration refers to the overall organization of a network in terms of connectivity and information transfer. A well-known measure of Integration is global efficiency. Segregation describes the formation of separate clusters within

a network or connectivity at a more regional level and an important measure is clustering coefficient. Lastly, Influence describes the importance of separate nodes within a network, which can be captured by computing centrality measures, such as betweenness and eigenvector centrality. Nodes that occupy a central position within the network are referred to as hub nodes (van den Heuvel & Sporns 2013). Damage to hub nodes, for example due to TBI, may have far-reaching effects on network function (Pandit et al. 2013).

Graph theory has proven powerful in revealing many (subtle) aspects of the pathophysiology of a wide range of neurological and psychiatric diseases (Filippi et al. 2013; Stam 2014). Quite recently, graph theory has been adopted as a method of studying functional and structural connectivity in patients with TBI (Caeyenberghs et al. 2012; Caeyenberghs et al. 2013; Caeyenberghs et al. 2014; Fagerholm et al. 2015; Kim et al. 2014; Messe et al. 2013; Nakamura et al. 2009; Pandit et al. 2013; Yuan et al. 2015). Studies on structural connectivity have included children and adolescents with acute (Yuan et al. 2015) and chronic mTBI (Caeyenberghs et al. 2012), and adult patients with chronic moderate-to-severe TBI (Caeyenberghs et al. 2013; Caeyenberghs et al. 2014; Fagerholm et al. 2015; Kim et al. 2014). These studies have shown changes in network Integration, Segregation and Influence. For example, lower global efficiency and higher clustering of structural networks was reported (Caeyenberghs et al. 2014; Yuan et al. 2015) as well as reduced centrality of hub nodes, such as the cingulate cortex (Fagerholm et al. 2015). Furthermore, lower global efficiency and centrality were found to be related to lower cognitive performance (Caeyenberghs et al. 2014; Fagerholm et al. 2015). Regarding adults with mild TBI, only one study on structural networks has been published thus far (Dall'Acqua et al. 2016). Using network based statistics (Zalesky et al. 2010), this study demonstrated reduced, predominantly frontal, structural connectivity in patients with high levels of self-reported symptoms. In addition, a graph theory study examined functional connectivity in patients with mTBI and reported changes in local measures, predominantly within the frontal and temporal regions, which were associated with post-traumatic complaints (Messe et al. 2013). Despite these interesting results, the structural connectome in patients with mTBI is still poorly understood.

The present study is the first to perform diffusion tractography followed by graph theory analysis in adult patients with uncomplicated (i.e. without abnormalities on CT) mTBI in the subacute phase after injury. Given the novelty of graph theory in the field of mild TBI, it is not straightforward which graph measures are most suitable for studying this condition. Therefore, an exploratory approach was used in the current study, and selection of graph measures was made, based on elaborate reviews of graph theory analysis (Fornito et al. 2013; Stam 2014; Rubinov & Sporns 2010; Sporns 2013) and previously published graph theory literature on

TBI (Caeyenberghs et al. 2012; Caeyenberghs et al. 2013; Caeyenberghs et al. 2014; Messe et al. 2013; Pandit et al. 2013; Fagerholm et al. 2015; Yuan et al. 2015). Graph measures related to Integration, Segregation and Influence were computed and the association with the presence or absence of post-traumatic complaints was examined. Because cognitive and affective complaints are among the most persistent complaints after mTBI (Dischinger et al. 2009; Ponsford et al. 2011), patients were selected who reported complaints within these domains. An additional research goal was to examine whether global and local graph measures in the subacute phase were predictive of cognitive performance at three months post-injury. In particular, it was examined whether global network measures were related to scores on tasks that measure processing speed.

Materials and methods

Study participants

Data from the patient group described in previously published fMRI research were used for the current diffusion weighted imaging (DWI) study (Harm J. van der Horn, Liemburg, Scheenen, et al. 2016). Fifty-three patients (18-65 years of age; 35 male) with mTBI were enrolled between March 2013 and February 2015 in the University Medical Center Groningen, the Netherlands (a level 1 trauma center). Mild traumatic brain injury was defined as a Glasgow Coma Score of 13-15 and/or loss of consciousness ≤ 30 minutes (Vos et al. 2002; Vos et al. 2012). The following exclusion criteria were used: lesions on admission CT scans, neurological and psychiatric co-morbidity, admission for prior TBI, drug or alcohol abuse, insufficient comprehension of Dutch language, mental retardation and contraindications for MRI (any implanted ferromagnetic devices and objects, pregnancy and/or claustrophobia). Furthermore, 20 healthy control (HC) subjects were recruited among social contacts and via advertisements, and group-matched with the total mTBI group for age, sex and educational level. Healthy controls had no history of traumatic brain injury.

Study approval was obtained from the local Medical Ethics Committee of the University Medical Center Groningen, the Netherlands, and all participants provided written informed consent after the study and procedure had been fully explained. All study procedures were carried out according to the declaration of Helsinki.

Clinical measures

At two weeks post-injury a post-traumatic complaints checklist comprised of 21 frequently occurring complaints was administered to patients. A detailed description of this questionnaire is available in previously published (de Koning et al. 2016;

van der Naalt et al. 1999). For the present study patients were selected based on the number of complaints and divided into two groups. Having post-traumatic complaints (PTC-present) (n=33; 17 male) was defined as reporting ≥ 3 complaints with at least one complaint in the cognitive and/or affective domain, and no complaints (PTC-absent) (n=20; 18 male) was defined as ≤ 2 complaints.

Healthy controls and patients (at \pm three months post-injury) also underwent neuropsychological testing. Since mental fatigue, concentration and memory problems are common complaints after mTBI, the following tests were applied: Trail Making Test A (processing speed) (Reitan & Wolfson 1985), Stroop I Test (verbal speed) (Hammes 1971), Digit-span Test backward (working memory) (Wechsler 2001) and the Dutch version of the Rey Auditory Verbal Learning Test (immediate and delayed verbal memory) (Rey 1964). Three patients did not return for neuropsychological follow-up. Raw scores, corrected for age and education level, were used for statistical analyses. To control for task under achievement, participants with a score < 85 on the Amsterdam Short Term Memory Test (Schmand et al. 1999) and/or > 5 on a brief version (neurological impairment and amnesic disorders subscales) of the Structured Inventory of Malingered Symptomatology (Smith & Burger 1997) were excluded from analyses. These participants included one HC and nine patients with mTBI (four PTC-absent and five PTC-present patients).

MRI acquisition

Participants underwent MRI scanning (patients at approximately four weeks post-injury) using a 3 T Philips Intera MRI scanner (Philips Medical Systems, Best, The Netherlands) equipped with a 32-channel SENSE head coil. For anatomical reference, a high resolution transversal T1-weighted image was acquired with the following parameters: repetition time (TR) 9 ms, echo time (TE) 3.5ms, flip angle 8° , field of view (FOV) 256x232 mm, voxel size 1x1x1 mm). Acquisition of diffusion weighted images was performed using single-shot echo planar imaging with the following parameters: TR 8884 ms, TE 60 ms, FOV 240x240 mm, acquisition matrix 96x95, 55 slices (thickness 2.5 mm), reconstructed voxel size 2.5x2.5x2.5 mm, 60 diffusion directions, b-value 1000 s/mm². In addition, 7 volumes without diffusion weighting (b=0 s/mm²) were acquired and averaged in a single volume by the MR-scanner.

For detection of post-traumatic lesions the following sequences were used: coronal T2*-gradient echo (TR 875ms, TE16ms, FOV 230x183mm, voxel size 0.90x1.12x4mm) and transversal susceptibility weighted imaging (TR 35ms, TE 15ms, FOV 230x183mm, voxel size 0.90x0.90x2mm). These sequences were examined for microbleeds (1-10mm) by an experienced neuroradiologist. Within the control group, no microbleeds were detected. Within the patient group, 28 percent showed ≥ 1 microbleeds. Seventy per cent of all lesions were located within

the frontal regions, 14% within the temporoparietal regions, 14% within other regions and 2% within the corpus callosum. No statistical differences in the presence ($\chi^2=0.046$, $P=0.831$) or number ($U=327$, $P=0.936$) of lesions were found between the PTC-present (median 0 lesions, range 0-37) and PTC-absent (median 0, range 0-26) groups.

Imaging data processing

Figure 1 shows the DWI and T1 processing pipeline. The T1-weighted scans were preprocessed using the recon-all function of FreeSurfer version 5.3 on a cluster of processors running Linux (Ubuntu 12.04.5 LTS, CPU model AMD Opteron Processor 6272). FreeSurfer starts with removing the non-brain tissue (Segonne et al. 2004) followed by automated Talairach transformation, segmentation of the subcortical white matter and deep gray matter volumetric structures (Fischl et al. 2002; Fischl, Salat, et al. 2004) and intensity normalization (Sled et al. 1998). It then proceeds with tessellation of the gray matter white matter boundary, automated topology correction (Fischl et al. 2001; Segonne et al. 2007) and surface deformation following intensity gradients to optimally place the gray/white and gray/cerebrospinal fluid borders at the location where the greatest shift in intensity defines the transition to the other tissue class (Dale & Sereno 1993; Dale et al. 1999; Fischl & Dale 2000). Finally, registration to a spherical atlas based on individual cortical folding patterns is performed (Fischl et al. 1999) followed by parcellation of the cerebral cortex into units with respect to gyral and sulcal structures (Fischl, van der Kouwe, et al. 2004; Desikan et al. 2006), which has shown to be a reliable way of defining subject specific regions of interest (ROIs). Default parameters were used for all processing steps. The quality of FreeSurfer results were examined in each subject by overlaying the subcortical segmentation and the white and pial surfaces on coronal, sagittal and axial T1 slices. The T1.mgz (i.e. the FreeSurfer T1 image) and aparc+aseg.mgz (i.e. image containing ROIs constructed by the FreeSurfer pipeline) files were converted to the nifti format (T1.nii and aparc+aseg.nii) to be used in further analyses.

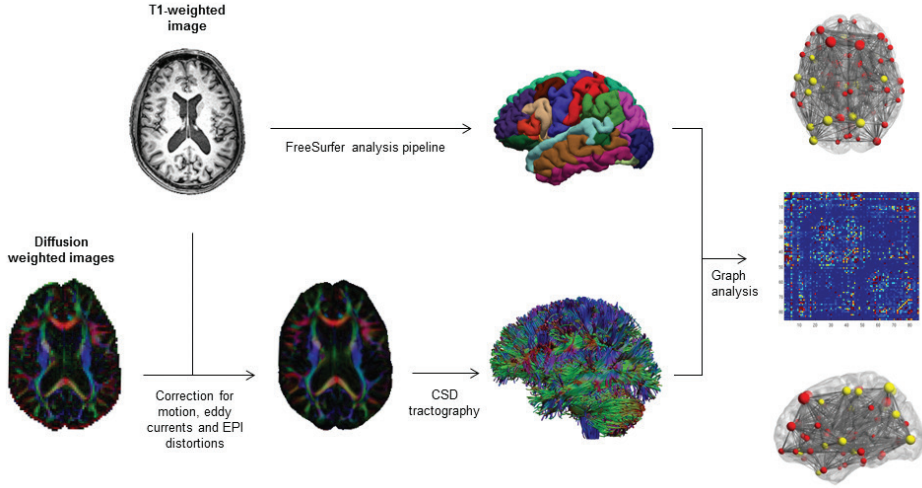


Figure 1: Data processing pipeline.

Diffusion data were processed using ExploreDTI (Leemans et al. 2009), version 4.8.5, using MATLAB (MATLAB Release 2014b, The MathWorks, Inc., Natick, Massachusetts, United States), which was run on a cluster of processors running Linux (CentOS 6.6, CPU model Intel Xeon E5 2680v3). First, the FreeSurfer T1.nii files were processed using the mask function from ExploreDTI, applying a kernel size of morphological operators of 5 and a threshold of 0.05. Subsequently, diffusion data were corrected for motion and eddy currents (Leemans & Jones 2009), and susceptibility distortions (Irfanoglu et al. 2012) with the masked T1.nii files as undistorted (target) scans, followed by constrained spherical deconvolution (CSD) tractography (Tournier et al. 2007; Jeurissen et al. 2011; Tax et al. 2014) resulting in one streamline file per subject. Default parameters were used for all processing steps in ExploreDTI, except for the aforementioned masking of the T1.nii file (because the applied parameters showed to result in proper masking results). The corrected diffusion results were quality checked in every subject by a) viewing all three planes of the diffusion weighted images in a movie loop, b) viewing the axial slices of the color coded FA map and c) viewing all three planes of the color coded FA map overlaid on the T1 volume.

Network construction

First, it was made sure that every ROI that was planned to be used in the analysis was present (i.e. “dissected”) in the aparc+aseg files of all subjects. The cerebellum, which was not fully covered in all scans, and the ventricles were excluded from the analysis,

resulting in 85 ROIs in each subject (see Supplementary Table 1). These comprised all cortical ROIs from the Desikan Killiany atlas (34 areas), plus Thalamus-Proper, Caudate, Putamen, Pallidum, Hippocampus, Amygdala, Accumbens-area and Ventral Diencephalon (all of them bilateral) and Brain-Stem. For each subject, these ROIs were combined with the information in the streamline file. For all possible ROI-pairs, the number of streamlines (> 0) between two ROIs was counted as all streamlines that had an endpoint in both ROIs (i.e., the 'END' option in ExploreDTI was used). The resulting number of streamlines were converted to square, symmetrical matrices (85 rows and 85 columns for all ROIs) and the main diagonal was set to zeros. These matrices were stored for subsequent network analysis.

Image quality assurance

Visual quality assurance of the FreeSurfer results yielded 12 scans that had to be (partially) rerun after some slight manual modifications. The final result was a proper delineation of all surfaces and subcortical ROIs in all subjects. Quality checking of the results of the ExploreDTI pipeline yielded no extra concerns in this regard, so all subjects could be used in further analyses.

Network analyses

Graph analysis was performed on weighted streamline matrices using the Brain Connectivity Toolbox (BCT) version 2016-16-01 (Rubinov & Sporns 2010) in combination with in-house developed MATLAB (v2011b) scripts. Graph measures were selected based on previously conducted graph theory studies on TBI. The following global (i.e. computed for the total network) measures were computed: global efficiency (E_{glob}), mean local efficiency (E_{loc}), normalized mean clustering coefficient (γ) and modularity (Q). Also, the following local (i.e. for individual nodes) measures were computed: nodes' degree (K_i), local efficiency (E_{loc_i}), clustering coefficient (C_i), betweenness centrality (BC_i) and eigenvector centrality (EC_i). Table 1 provides a description of all measures used in the current study, categorized by domain of network organization (Integration, Segregation and Influence (Rubinov & Sporns 2010; Sporns 2013)). For a detailed description of these measures we refer

Table 1: Graph measures.

| Measure | Description |
|--|---|
| Integration: | |
| Global efficiency (E_{glob}) | This global measure is calculated by taking the mean inverse shortest pathlength in the network. E_{glob} is inversely related to the characteristic pathlength of the total network (i.e. networks with high E_{glob} have short pathlengths between nodes). |
| Segregation: | |
| Clustering coefficient (C_i) | Fraction of triangles around a node (i.e. fraction of neighbors of node i that are neighbors of each other). This measure reflects the tendency of nodes to cluster together. |
| Mean clustering coefficient (C) | This global measure is calculated by taking the mean of clustering coefficients of all individual nodes in the network. |
| Normalized clustering coefficient (γ) | Mean clustering coefficient divided by the clustering coefficient of a random null network with preserved degree distribution. |
| Local efficiency (E_{loc}) | Efficiency of connections between (1st degree) neighbors of a node (i.e. E_{loc} reflects the global efficiency of the neighborhoods of node i). |
| Mean local efficiency (E_{loc}) | This global measure is calculated by taking the mean of local efficiency values of all nodes in the network. |
| Modularity (Q) | This global measure quantifies the degree to which a network may be subdivided into modules (i.e. sub-networks consisting of non-overlapping groups of nodes). |
| Influence: | |
| Degree (K_i) | Number of edges connected to a node. |
| Betweenness centrality (BC_i) | Fraction of all the shortest paths in the network that pass through a certain node. Nodes with high BC_i are said to be hub nodes. |
| Eigenvector centrality (EC_i) | Self-referential measure that reflects how strong node's neighbors are connected. High EC_i indicates that node i is connected to important nodes. |

the reader to the paper by Rubinov and Sporns (Rubinov & Sporns 2010). Since there exist inter-individual variations in whole brain number of reconstructed streamlines, for example due to sex and age differences (Gong et al. 2009), prior to graph analysis connectivity matrices were normalized using the BCT weight conversion function. Subsequently, graph measures were computed over a range of network density thresholds (0.01-0.28, with increments of 0.01, obtained using the BCT threshold proportional function), aimed at reducing the influence of spurious connections. A range of thresholds was used to avoid unwanted modifications of graph measures that may occur when using a fixed threshold (van Wijk et al. 2010). The upper limit was set at 0.28, at which all participants' connectivity matrices showed maximum density (i.e. unthresholded matrices). To obtain a scalar that was independent of selecting a single threshold, the area under the curve (AUC) was calculated across thresholds for every subject. These values were used for statistical group analyses.

Statistical analyses

Analyses of demographics and clinical measures were conducted using the statistical package for Social Sciences (SPSS; version 22.0; Armonk, NY: IBM Corp). Data were assessed for normality using Shapiro-Wilk tests. Normally distributed continuous variables were analyzed using one-way analysis of variance (ANOVA) and two-sample t-tests. Non-normally distributed continuous variables were analyzed using Kruskal-Wallis and Mann-Whitney *U* tests. Pearson's chi-square tests were used for categorical variables. Group comparisons of neuropsychological test scores were performed using analysis of covariance with inclusion of age and education level as covariates.

Permutation tests (10,000 random permutations) were conducted in MATLAB (v2011b) to assess differences in AUC values of global and local graph measures between mTBI patients and HC, between patients with and without PTC, and between each of the patient subgroups separately and HC. Group differences in global measures were considered significant at a false discovery rate (FDR) of 0.05 (number of global measures was 4) (Benjamini & Hochberg 1995). Each of the local measures were deemed significant at the same FDR of 0.05 (number of nodes was 85). In addition, the common language effect size indicator (CL) was calculated to estimate effect sizes (McGraw & Wong 1992). Since there was a difference in the ratio of male to female subjects between patients with and without complaints, global and/or local graph measures that were significantly different between these groups were also compared between male and female patients (with a FDR of 0.05). This comparison was made within the PTC-present group only, since the PTC-absent group contained only two female patients. To account for a potential influence of microbleeds, global and local graph measures were also compared between patients

with and without lesions (with a FDR of 0.05).

Using MATLAB, partial Spearman's rank correlations were computed between graph AUC values and neuropsychological test scores in the total group of mTBI patients with correction for age and education level. For the global network measures (Eglob, mean Eloc, γ and Q), correlations were computed between AUC values and scores on tests measuring processing speed (TMT-A and Stroop I). In addition, it was assessed whether local graph measures of specific nodes were associated with scores on verbal memory (RALVT) and verbal working memory (Digit-span backward) tests. Nodes were selected based on the cognitive domains that were assessed by the specific tests. Hence, correlations were computed between graph AUC values of temporal nodes + the opercular and triangular parts of the inferior frontal gyri (i.e. Broca's area) and RALVT scores, and between AUC values of frontoparietal nodes and Digit-span Test backward scores (node selections are listed in Suppl. Table 1). Again, results were considered significant at a FDR of 0.05 (i.e. corrected for the number of global measures or nodes).

Results

Demographics and clinical characteristics

Demographics and clinical characteristics of this study population are listed in Table 2. The total group of patients with mTBI was matched with HC on age, sex, education level and handedness. Injury and other characteristics were similar for PTC-present and PTC-absent patients, except for sex ($\chi^2=8.224$; $P=0.004$). Regarding neuropsychological tests, no differences were found between patients with mTBI and HC when adjusting for age and education level. However, PTC-present patients had lower scores (indicating better performance) on TMT-A than PTC-absent patients ($F=5.94$, $P=0.02$). Regarding cognitive complaints, fatigue was reported by 91% of the PTC-present group, forgetfulness and (mental) slowness by 78%, and poor concentration by 73%. One patient in the PTC-absent group reported fatigue and no other cognitive complaints were reported in this group.

Table 2: Participant characteristics.

| | PTC-present (n=33) | PTC-absent (n=20) | HC (n=20) | P-value |
|---|--------------------|-------------------|--------------|--------------------|
| Age, median (range), years | 33 (19-63) | 34 (20-64) | 30 (18-61) | 0.935 ^a |
| Sex, % male | 52 | 90 | 70 | 0.015 ^b |
| Education level, median (range) ^c | 6 (4-7) | 6 (2-7) | 6 (5-7) | 0.350 ^b |
| Handedness, % right | 91 | 80 | 85 | 0.524 ^b |
| Interval injury to MRI, median (range), days | 32 (22-56) | 33 (22-69) | N/A | 0.526 ^d |
| Interval injury to two-week questionnaire, median (range), days | 14 (10-31) | 13 (10-58) | N/A | 0.830 ^d |
| GCS score, median (range) | 14 (13-15) | 15 (13-15) | N/A | 0.072 ^b |
| Post-traumatic amnesia, % yes | 91 | 70 ^e | N/A | 0.097 ^b |
| Injury mechanism: | | | | |
| Traffic, % of group | 52 | 50 | N/A | 0.915 ^b |
| Falls, % | 39 | 45 | N/A | 0.547 ^b |
| Sports, % | 3 | 0 | N/A | 0.420 ^b |
| Assault, % | 3 | 0 | N/A | 0.420 ^b |
| Other, % | 3 | 5 | N/A | 0.727 ^b |
| Neuropsychological tests: | n=24 | n=17 | n=19 | |
| TMT-A, mean (range) | 22.8 (14-44) | 30.5 (14-57) | 26.5 (12-43) | 0.043 ^f |
| Stroop I, mean (range) | 42.6 (30-58) | 45.4 (31-72) | 45.2 (26-71) | 0.552 ^f |
| Digit-span backward, mean (range) | 5.3 (3-9) | 5.2 (2-8) | 5.3 (3-8) | 0.936 ^f |
| RAVLT | | | | |
| Immediate recall, mean (range) | 48.8 (17-65) | 46 (31-69) | 48.6 (32-71) | 0.746 ^f |

| Delayed recall, mean (range) | 10.1 (2-15) | 10.1 (6-14) | 10.2 (3-15) | 0.985 ^f |
|------------------------------|-------------|-------------|-------------|--------------------|
|------------------------------|-------------|-------------|-------------|--------------------|

^aKruskal-Wallis test; ^bPearson's chi-square test; ^cEducation level was based on a Dutch classification system, according to Verhage (Verhage F (1964): *Intelligence and age: Study with Dutch people from age 12 to 77. Dissertation Van Gorcum, Assen, The Netherlands*), ranging from 1 to 7 (7 being highest); ^dMann-Whitney U test; ^ePost-traumatic amnesia was documented for 95% of the PTC-absent patients; ^fANCOVA with covariates age and education level.

Abbreviations: GCS = Glasgow Coma Score; MRI = Magnetic Resonance Imaging; N/A = not applicable; PTC = post-traumatic complaints; RALVT = Rey Auditory Verbal Learning Test; TMT = Trail Making test.

Group differences in global network measures

In Figure 2, global measures are depicted across thresholds for the two patient subgroups and HC. There were no differences in AUC values between patients with mTBI and HC. Significantly lower AUC values were found in PTC-absent patients compared to PTC-present patients for Eglob ($P_{\text{uncorrected}} = 0.0074$; $P_{\text{FDR}} = 0.0258$; CL = 0.71) and Eloc ($P_{\text{uncorr.}} = 0.0129$; $P_{\text{FDR}} = 0.0258$; CL = 0.69). A trend was found toward higher values of γ in PTC-absent patients ($P_{\text{uncorr.}} = 0.08$; CL = 0.36). Regarding Q, AUC values did not differ significantly between patient subgroups ($P_{\text{uncorr.}} = 0.45$). For none of the global measures, differences were found when comparing patient subgroups separately to HC.

Secondary analyses showed no significant differences between male and female patients in the PTC-present group for AUC values of Eglob and Eloc. Furthermore, no differences were found between patients with and without microhemorrhagic lesions.

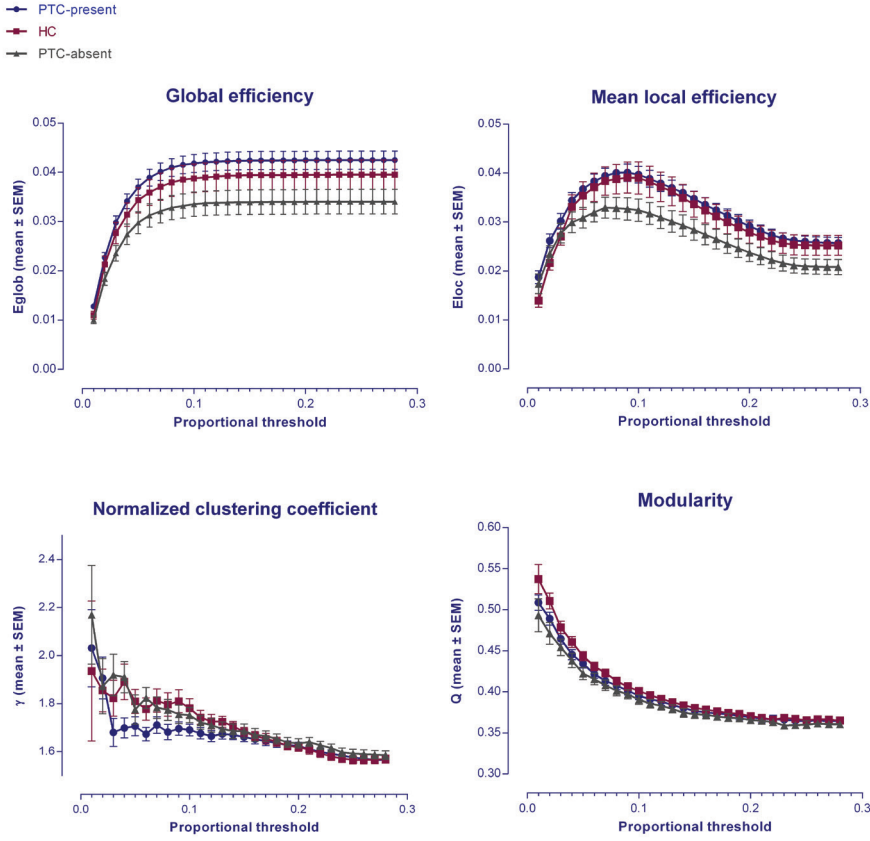


Figure 2: Global network measures across density thresholds for patients with (PTC-present) and without (PTC-absent) post-traumatic complaints and healthy controls (HC).

Group differences in local network measures

Regarding most of the local measures, no significant differences were present between patients with mTBI and HC, or between patient subgroups. However, AUC values for ECI of the left temporal pole were found to be significantly lower in both the total group of patients with mTBI ($P_{\text{uncorr.}} = 0.0001$; $P_{\text{FDR}} = 0.0085$; CL = 0.31) and the PTC-present subgroup separately ($P_{\text{uncorr.}} = 0.0002$; $P_{\text{FDR}} = 0.0170$; CL = 0.3) compared to HC (Fig. 3). A trend towards lower ECI of the orbital part of the left inferior frontal gyrus was found in mTBI patients compared to HC ($P_{\text{uncorr.}} = 0.0013$, $P_{\text{FDR}} = 0.055$; CL = 0.3).

No differences in local measures were found between patients with and without microhemorrhagic lesions.

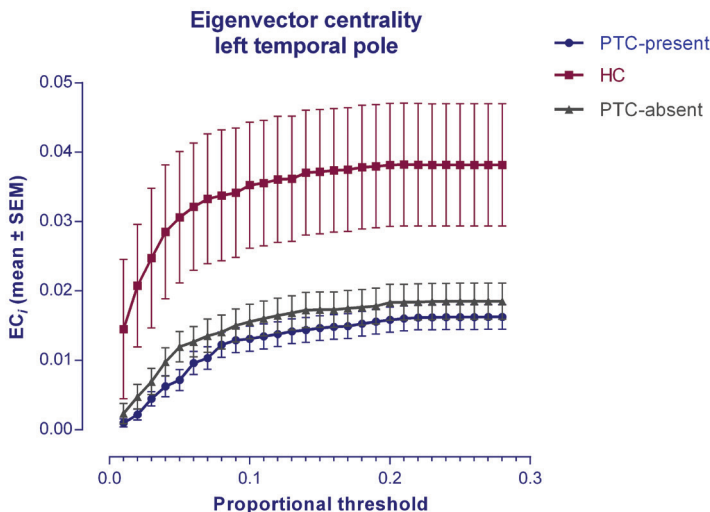


Figure 3: Eigenvector centrality (EC_i) of the left temporal pole across density thresholds in healthy controls and patients with (PTC-present) and without (PTC-absent) complaints.

Associations between graph measures and neuropsychological tests

Within the mTBI group there was a partial correlation observed at trend level between higher γ values and higher TMT-A scores corrected for age and education level ($\rho = 0.31$, $P_{\text{uncorr.}} = 0.05$; $P_{\text{FDR}} = 0.22$). In other words, lower network clustering corresponded to higher processing speed. Regarding local measures in the mTBI group, there was a significant negative partial correlation between BC_i values of the opercular part of the left inferior frontal gyrus and immediate recall scores on the RAVLT ($\rho = -0.57$, $P_{\text{uncorr.}} = 0.0001$; $P_{\text{FDR}} = 0.006$); and between BC_i values of left superior temporal gyrus and delayed recall scores on the RAVLT ($\rho = -0.49$, $P_{\text{uncorr.}} = 0.002$; $P_{\text{FDR}} = 0.03$). Thus, higher betweenness centrality of these nodes corresponded with lower memory performance.

Discussion

This is the first study that has applied graph theory analysis to structural networks (reconstructed from DWI data) in a large sample of adult patients with uncomplicated mTBI. Global measures were similar when comparing the total mTBI group with healthy controls. Within the mTBI group, patients without post-traumatic complaints had lower global measures (Eglob and Eloc) compared to patients with complaints. For local measures, lower eigenvector centrality within the left temporal pole was found in patients with mTBI compared to healthy controls, possibly reflecting temporal lobe injury. Neuropsychological performance was similar for patients with mTBI and healthy controls. Nevertheless, in patients with mTBI a trend was found towards a relationship between lower network clustering and higher processing speed, and this finding was associated with post-traumatic complaints. More specifically, our findings might indicate a (compensatory) shift towards a more random network configuration in patients with complaints, possibly facilitating faster information transfer throughout the network. Additionally, higher betweenness centrality of areas involved in language processing was related to poorer memory performance, which may suggest a possible compensatory role for language hubs in patients with post-mTBI memory problems.

The use of graph theory to study structural brain networks obtained from DWI has increased rapidly over the past few years, in the field of traumatic brain injury as well. Studies have reported differences regarding various graph measures between patients with chronic moderate-to-severe TBI and healthy controls, showing that lower global efficiency and centrality values were associated with worse cognitive performance (Caeyenberghs et al. 2014; Kim et al. 2014; Fagerholm et al. 2015). These studies suggest that changes in structural network configuration may explain deficits following more severe TBI. To date, only one study has investigated the structural connectome in adult patients with mTBI using network based statistics (Dall'Acqua et al. 2016). In this study, whole-brain structural connectivity (number of streamlines) was found to be similar for both patients with acute mTBI (with on average three symptoms) and healthy controls. In the present study, several graph measures were compared between patients with mTBI and healthy controls, which to our knowledge was done here for the first time. One local measure, namely eigenvector centrality of the left temporal pole, was lower in patients with mTBI compared to healthy controls. Eigenvector centrality is a self-referential measure that reflects the level of importance (hub status) of the neighbors of a node. This could mean that connectivity of hub nodes adjacent to the temporal pole was disturbed in patients with mTBI, which can be explained given the vulnerability of this area to TBI (Bigler 2007). Although eigenvector centrality of other vulnerable areas, such as the frontal lobes, was similar for patients and healthy controls, we did find a trend towards lower eigenvector centrality of the left inferior frontal gyrus in the mTBI

group. In patients with moderate to severe TBI, reduced eigenvector centrality of hub regions, such as the cingulate cortex, has been reported (Fagerholm et al. 2015). However, this was not found in the current study. Moreover, global measures were also similar in the total group of patients with mTBI and healthy controls, which might indicate that mTBI causes minor local network changes that do not affect global network functioning. Another possible explanation for these findings may be the time interval between injury and scanning, which in the current study was approximately 30 days. A study by Yuan *et al.* has shown that global efficiency of structural networks in children and adolescents with mTBI (within 96 hours post injury) was lower compared to healthy controls, which may suggest that changes in structural networks are more prominent in the acute phase (Yuan et al. 2015). However, it also has to be taken into account that the brains of young patients with mTBI may be more vulnerable to injury compared to those of adult patients considering ongoing developmental processes (Lenroot & Giedd 2006).

Recent studies using non-graph theory methods on DTI data did not demonstrate differences between adult patients with and without complaints in the acute and subacute stages after mTBI (Ilvesmaki et al. 2014; Wäljas et al. 2014; Lange et al. 2015). The present study showed that, using CSD tractography and graph theory, it is possible to discern differences in structural network connectivity between patients with and without post-traumatic complaints in the subacute phase post-mTBI. Patients without complaints had lower values on global measures of network integration (Eglob) and segregation (Eloc) compared to patients with complaints, while local measures did not differ. Contrary to our results, a recent study has shown that reduced frontal structural network connectivity (number of streamlines) was associated with higher levels of symptoms reported acutely after mTBI (Dall'Acqua et al. 2016). Moreover, one graph theoretical study on functional networks showed only a relationship between local graph measures of frontotemporal regions and post-traumatic complaints in mTBI without any significant findings regarding global measures (Messe et al. 2013). Remarkably, our findings also demonstrated that network measures in both the group of patients with and the group without complaints did not differ significantly from healthy controls, which might imply that the injury itself does not cause major perturbations in the structural network in patients with mTBI. An exciting idea is that differences in structural connectivity may be related to pre/non-injury related factors, such as personality characteristics, which may explain differences in susceptibility to develop (persistent) complaints. In healthy subjects, for example, it has been demonstrated that a more random functional network in terms of higher global efficiency was related to higher scores on a neuroticism questionnaire (Servaas et al. 2015). Since it was found that patients with complaints had higher global efficiency compared to patients without complaints, it could be hypothesized that neuroticism also plays a role in developing

complaints after mTBI.

Although several cognitive complaints were reported by patients with mTBI, performance scores on neuropsychological tests at follow-up fell within the normal range, which is consistent with the existing literature (Carroll et al. 2004; Carroll et al. 2014; Rohling et al. 2011). Mental fatigue is commonly reported after mTBI, also in the current patient sample, and this complaint has been found to be related to processing speed in patients with acute and chronic mTBI (Johansson et al. 2009; Liu et al. 2016). In the present study, a trend was found towards a moderate correlation between better (faster) performance on the TMT-A and lower network clustering in the group of mTBI patients, which might be reflective of an early compensatory process to ensure adequate cognitive performance in the long term. Interestingly, patients with complaints performed better on the TMT-A compared to those without complaints, which might be related to (compensatory) increased mental effort and subsequent mental fatigue. Our results also show a trend toward lower network clustering in patients with complaints, compared to those without complaints. Although speculative, these findings may complement fMRI studies that have found higher activation during working memory processing in patients with mTBI compared to healthy controls, which was also thought to be associated with enhanced mental effort to maintain normal task performance (McAllister et al. 1999; McAllister et al. 2001). In addition, we found a significant association between lower scores on a verbal memory task and higher BCI of language areas in the left hemisphere, which might also reflect a compensatory process via increased usage of the phonological loop in patients with mTBI (Buchsbaum & D'Esposito 2008). Perhaps more important, hub-status of these nodes appears to be predictive of memory processing at follow-up. Further studies are required to elucidate the association between structural networks and cognitive outcome after mTBI.

Most of the DTI studies on mTBI so far have used voxel-based or ROI analyses and none have used graph theory. A systematic review of the literature has shown that results of these studies vary significantly regarding the presence or absence of diffusion abnormalities, direction (e.g. increased or decreased FA or MD) and anatomical location of abnormalities, and associations with neuropsychiatric complaints in patients with mTBI (Dodd et al. 2014). The authors report that these mixed results may be partly attributed to the heterogeneous nature of mTBI itself and of patient samples included in these studies (e.g. number of patients, injury severity and time post-injury). Furthermore, they found that data acquisition parameters are of influence. For example, a low number of diffusion weighted images (<20) may lead to more variable results. The current study has several methodological strengths that deal with these concerns. First, in comparison to several other studies, sufficient sample size was used and attempts were made to reduce heterogeneity (e.g. matching injury-to-scanning intervals of mTBI subgroups). Second, a high number

of diffusion weighted images was acquired (i.e. 60). Third, whereas many studies so far have used DTI tractography, here CSD tractography was used, which is capable of identifying crossing fiber tracts, resulting in fewer “false negative tracts” (Tournier et al. 2007).

There are also some limitations that should be mentioned. First, the b-value applied (1000 s/mm²) in the present study is relatively low for CSD, in which higher b-values are able to resolve crossing fibers at even lower angles. Second, the reader should not delude him- or herself that by weighting the connectivity matrices for streamline count, the number of axons was directly investigated (which could be considered a measure of white matter connection strength). The number of streamlines can be affected by a multitude of uninteresting and biologically irrelevant factors in addition to the actual number of underlying axons/tracts (Jones 2010; Jones et al. 2013). Rather, streamline sets were constructed in the diffusion field, of which it is known that “false positive tracts” (i.e. streamlines that were found, but should not have been reconstructed if it were for the underlying white matter) and “false negative tracts” are present in addition to “true positive tracts”, leading to the proper conclusion that we were at best investigating indirect measures of connection strength. Nevertheless, it has been shown that within-subject similarity of diffusion tractography network measures is higher than between-subject similarity (Bassett et al. 2011), and thus current findings are probably reflective of various biological processes. To date, no other methods have been developed that come near the method of diffusion tractography regarding the reconstruction of “fiber tracts” in vivo, especially when it comes to whole-brain connectivity. Third, there is no consensus regarding many of the choices that have to be made with (DWI) graph analysis (e.g. regarding parcellation of the brain, selection of streamlines that pass through or end in an ROI, normalization of weighted matrices, graph thresholding and multiple comparison correction (Duarte-Carvajalino et al. 2012; Fornito et al. 2013)), and results may vary accordingly. Fourth, imaging was performed in the subacute phase post-injury only, and not acutely after injury as well. Therefore, we were not able to determine whether our findings (also) reflected possible compensatory processes to acute injury. Lastly, although the current study provides novel perspectives on mTBI, replication studies are needed to demonstrate the reliability of our findings.

In conclusion, this study has demonstrated relatively minor differences in graph properties of the structural connectome in patients with uncomplicated mTBI when compared to healthy controls. Interestingly, within the mTBI group, values of global and local efficiency were lower in patients without complaints compared to patients with complaints, while both patient subgroups did not differ from healthy controls. Possible indications were found for early compensatory mechanisms in patients with mTBI involving network clustering and betweenness centrality of language areas to ensure adequate cognitive performance at follow-up. Diffusion

weighted structural graph analysis in neuroscience is still in its infancy, but it is a promising tool in further disentangling the role of structural injury in uncomplicated mTBI, possibly leading to clinically relevant clues for future diagnostics and treatment of patients with mTBI.

Supplementary Table 1: Regions of interest for network analyses (ROIs total) and selection of ROIs for correlation with Rey Auditory Verbal Learning Test (RAVLT) and Digit-span backward.

| ROIs total | ROIs RAVLT | ROIs Digit-span backward |
|-------------------------------------|--------------------------------------|----------------------------------|
| Left Thalamus Proper | Left Hippocampus | Left caudal anterior cingulate |
| Left Caudate | Right Hippocampus | Left caudal middlefrontal |
| Left Putamen | Left fusiform | Left inferior parietal |
| Left Pallidum | Left inferior temporal | Left pars opercularis |
| Brain Stem | Left middle temporal | Left pars triangularis |
| Left Hippocampus | Left parahippocampal | Left precuneus |
| Left Amygdala | Left pars opercularis | Left rostral anterior cingulate |
| Left Accumbens area | Left pars triangularis | Left rostral middle frontal |
| Left Ventral Diencephalon | Left superior temporal | Left superior frontal |
| Right Thalamus Proper | Left supramarginal | Left superior parietal |
| Right Caudate | Left temporal pole | Left frontal pole |
| Right Putamen | Left transverse temporal | Right caudal anterior cingulate |
| Right Pallidum | Right fusiform | Right caudal middle frontal |
| Right Hippocampus | Right inferior temporal | Right inferior parietal |
| Right Amygdala | Right middle temporal | Right pars opercularis |
| Right Accumbens area | Right parahippocampal | Right pars triangularis |
| Right Ventral Diencephalon | Right pars opercularis | Right precuneus |
| Left banks superior temporal sulcus | Right pars triangularis | Right rostral anterior cingulate |
| Left caudal anterior cingulate | Right superior temporal | Right rostral middle frontal |
| Left caudal middle frontal | Right supramarginal | Right superior frontal |
| Left cuneus | Right temporal pole | Right superior parietal |
| Left entorhinal | Right transverse temporal | Right frontal pole |
| Left fusiform | Left banks superior temporal sulcus | |
| Left inferior parietal | Right banks superior temporal sulcus | |
| Left inferior temporal | | |
| Left isthmus cingulate | | |
| Left lateral occipital | | |
| Left lateral orbitofrontal | | |
| Left lingual | | |
| Left medial orbitofrontal | | |
| Left middle temporal | | |

| |
|--------------------------------------|
| Left parahippocampal |
| Left paracentral |
| Left pars opercularis |
| Left pars orbitalis |
| Left pars triangularis |
| Left pericalcarine |
| Left postcentral |
| Left posterior cingulate |
| Left precentral |
| Left precuneus |
| Left rostral anterior cingulate |
| Left rostral middle frontal |
| Left superior frontal |
| Left superior parietal |
| Left superior temporal |
| Left supra marginal |
| Left frontal pole |
| Left temporal pole |
| Left transverse temporal |
| Left insula |
| Right banks superior temporal sulcus |
| Right caudal anterior cingulate |
| Right caudal middle frontal |
| Right cuneus |
| Right entorhinal |
| Right fusiform |
| Right inferior parietal |
| Right inferior temporal |
| Right isthmus cingulate |
| Right lateral occipital |
| Right lateral orbitofrontal |
| Right lingual |
| Right medial orbitofrontal |
| Right middle temporal |
| Right parahippocampal |

| |
|----------------------------------|
| Right paracentral |
| Right pars opercularis |
| Right pars orbitalis |
| Right pars triangularis |
| Right pericalcarine |
| Right postcentral |
| Right posterior cingulate |
| Right precentral |
| Right precuneus |
| Right rostral anterior cingulate |
| Right rostral middle frontal |
| Right superior frontal |
| Right superior parietal |
| Right superior temporal |
| Right supramarginal |
| Right frontal pole |
| Right temporal pole |
| Right transverse temporal |
| Right insula |

